Journal of Catalysis **203,** 94–103 (2001)
doi:10.1006/jcat.2001.3237, available online at http://www.idealibrary.com on IDEAL®

In Situ Characterization of Sn–Pt/SiO_2 Catalysts Used in Low Temperature Oxidation of CO

J. L. Margitfalvi,[1] I. Borbáth, K. Lázár,* E. Tfirst, A. Szegedi, M. Hegedűs, and S. Gőbölös

*Institute of Chemistry, Chemical Research Center, Hungarian Academy of Sciences, 1025 Budapest, Pusztaszeri út 59-67, Hungary; and *Institute of Isotope and Surface Chemistry, Chemical Research Center, Hungarian Academy of Sciences, 1525 Budapest, POB 77, Hungary*

Received December 20, 2000; revised March 26, 2001; accepted March 26, 2001

Sn–Pt/SiO_2 catalysts used in room temperature oxidation of CO were characterized by *in situ* techniques applying both Mössbauer and FTIR spectroscopy. The catalysts were prepared by an organometallic method (CSR) using $^{119}Sn(CH_3)_4$. The Mössbauer spectra revealed the presence of platinum-rich [PtSn(a)] and tin-rich [PtSn(b)] alloy species as the main tin-containing components accounting for more than 85% of tin after activation of the catalysts in hydrogen at 573 K. The results of Mössbauer spectroscopy showed that the oxidation of the less stable tin-rich PtSn(b) component, with looser Sn–Pt bonds, is primarily involved in surface reactions taking place in the low temperature CO oxidation. The oxidation of both PtSn(b) and PtSn(a) species leads to the formation of new species and sites, such as (i) a tin oxide phase, (ii) a mobile Sn^{4+}(sf) species, (iii) platinum sites, and (iv) the appearance of a third alloy species, PtSn (1 : 1). The net result of this transformation is the formation of highly active "*Sn^{4+}–Pt*" *ensemble* sites, where Sn^{4+} sites are in the atomic closeness of Pt. In both CO oxidation and subsequent reactivation in hydrogen a reversible PtSn(b) ↔ Sn^{4+} + Pt interconversion takes place at room temperature. The probability of the Mössbauer effect, f_A (approximated by $d\ \ln(A_{300}/A_{77})/dT$), indicates the surface location of the involved components. The results of *in situ* FTIR spectroscopy provided further proof for the above interconversion and unambiguous evidences of the involvement of both Pt-rich PtSn(a) and Sn-rich PtSn(b) alloy species in the above interconversion. The catalytic experiments are in full accordance with the results of spectroscopic measurements. The possible mode of activation of the CO molecule over the (110) surface of the PtSn (1 : 1) alloy was also modeled and calculated.

Key Words: in situ **spectroscopy; Sn–Pt/SiO_2 catalysts; low temperature CO oxidation; Mössbauer spectroscopy; FTIR; Sn^{4+}–Pt ensemble sites; density functional calculations.**

INTRODUCTION

Pt/SnO_2 (1–5) and Pd/SnO_2 (6, 7) catalysts are widely used as low temperature CO oxidation catalysts. Recently we have shown that alloy-type Sn–Pt/SiO_2 catalysts prepared by using anchoring-type controlled surface reactions (CSRs) between tin tetraalkyls and hydrogen adsorbed on platinum are highly active in this reaction (8). The activity of the Sn–Pt/SiO_2 catalysts strongly depended on the Sn/Pt ratio and catalysts with Sn/Pt ratio between 0.4 and 0.7 had the highest activity. Based on our recent catalytic and Mössbauer spectroscopy results (8) and the mechanism presented in Ref. (5) we have suggested that the activation of the CO molecule can be related to (i) the atomic closeness of Pt and Sn^{4+} sites formed *in situ* during the oxidation, and (ii) the C≡O–Sn^{4+} interaction. Accordingly, in the activation of CO the "*Sn^{4+}–Pt*" *ensemble* sites formed *in situ* from supported Pt–Sn nanoclusters should be involved (8). This suggestion has been supported by the results of *ab initio* Hartree-Fock calculations carried out for the C≡O–Sn^{4+} interaction (8).

Based on results of *in situ* Mössbauer spectroscopy the formation of similar types of sites has been suggested in the selective hydrogenation of crotylaldehyde to crotylalcohol (9). Consequently, the activation of the CO molecule and the carbonyl group showed distinct similarities. In both cases the activation is due to the C≡O–Sn^{4+} or >CO=O–Sn^{4+} interaction over the Sn^{4+}–Pt ensemble sites.

In this paper we provide further *in situ* spectroscopic evidence for the formation of Sn^{4+}–Pt ensemble sites upon investigation of the transformation of supported Pt–Sn alloy species in the presence of a CO and oxygen mixture at room temperature. In addition, an attempt was made in this study to model and calculate the interaction of adsorbed CO molecule with hypothetical Sn^0–Pt and Sn^{4+}–Pt ensemble sites.

EXPERIMENTAL

A 3% Pt/SiO_2 catalyst (CO/Pt = 0.52) was used as a parent catalyst. Tin tetramethyl ($^{119}Sn(CH_3)_4$) was applied as tin precursor compound. The tin anchoring was carried out in benzene at 323 K in a hydrogen atmosphere for 2 h. Details of surface chemistry involved in this type of catalyst modification can be found elsewhere (10, 11). The decomposition of multilayer organometallic complex

[1] To whom correspondence should be addressed. Fax: 36-1-325-7554. E-mail: joemarg@cric.chemres.hu.

0021-9517/01 $35.00

(MLOC) was accomplished in both oxidative and reductive atmospheres by the temperature programmed reaction (TPRe) technique (heating rate = 5 K/min, temperature ramp from 295 to 613 K). The use of reductive atmosphere provides alloy-type Pt–Sn nanoclusters (12, 13), while the oxidative one should give finely dispersed SnO_x ($x = 2$ or 4) over platinum (11, 13). These two types of catalysts are distinguished as (H)- and (O)-type catalysts, respectively. In both types of Sn–Pt/SiO_2 catalysts after reduction at 613 K the tin–platinum alloy phases are the main components and the amount of ionic forms of tin is less than 10% (13). In this study the following catalysts were prepared and used: Sn–Pt/SiO_2 (A) (Sn/Pt (at./at.) = 0.19, CO/Pt = 0.30) and Sn–Pt/SiO_2 (B) (Sn/Pt (at./at.) = 0.68, CO/Pt = 0.20, Catalyst No. II-3 in Ref. (8)). Chemisorption measurements using CO were done using ASDI RXM–100 equipment. In time-on-stream (TOS) experiments, a gas mixture containing 1.5 vol% CO and 0.64 vol% oxygen in helium was applied. In these experiments the space velocity was 24,000 ml $(g_{cat})^{-1}$ h^{-1}. Prior to the reaction the catalysts were rereduced at 613 K for 1.5 h in a hydrogen atmosphere (flow rate 60 ml/min).

Mössbauer spectra were recorded at 300 and 77 K with a constant acceleration spectrometer using a $Ba^{119}SnO_3$ source. All isomer shifts were referred to SnO_2. A standard least-squares minimization routine was used to fit the spectra as a superposition of Lorentzian lines. From spectra recorded at 300 and 77 K, $f_A = d\ \ln(A_{300}/A_{77})/dT$ data were also calculated, where A_{300} and A_{77} are the actual absorption areas of components in the spectra recorded at 300 and 77 K, respectively. f_A is connected to the probability of the Mössbauer effect; it provides a rough estimation for the bonding strength of the particular species (the smaller f_A is the stronger the bond). The catalyst samples were treated *in situ* and measured in the Mössbauer cell (14). The duration of treatment in a hydrogen atmosphere at 573 K was 90 min. The *in situ* experiments were carried out at room temperature at a constant flow of $CO : O_2$ (1 : 1) mixture (2 ml/min for 1.5 h).

In situ infrared spectra were obtained at room temperature using a Nicolet Impact 400 FTIR instrument. In the spectral range of 2200–1700 cm^{-1} two bands were detected. The high intensity one corresponds to the linearly chemisorbed CO, while the low intensity broad band is characteristic for bridged CO. In the spectral region 2200–1900 cm^{-1} the resolution was 1 cm^{-1}; however, due to the low intensity and the strong broadening the resolution of the bridged CO was in the range of 4 cm^{-1}. The description of the cell and the high vacuum apparatus used can be found elsewhere (15). Catalyst samples were ground-sieved and pressed onto self-supporting disks and mounted in the sample holder. The weight of the self-supporting disks was about 2.5–4.0 mg/cm^2. The calculated band intensities were corrected for the weight of the sample. The band intensities were determined by integration in the 1985–2125 and 1750–1925 cm^{-1} range, and the relative error of integration is 5 and 15% for the linear and the bridged carbonyl groups, respectively. The treatment of the sample was accomplished in a heated attachment chamber located above the IR cell. The catalysts were rereduced in hydrogen at 613 K for 2 h followed by evacuation at the same temperature for 1 h and cooling to room temperature under vacuum (10^{-3} mbar). FTIR spectra were measured at 10 Torr (13.5 mbar) CO and 5 Torr (6.7 mbar) oxygen pressure, i.e., under conditions used earlier in time-on-stream experiments (8). The spectra were obtained after accumulation of 200 scans. First the background spectra were measured, followed by the introduction of 10 Torr CO. In the presence of CO spectra were taken after 8, 24, and 40 min. Spectra taken after 40 min were used for comparison. In the next step 5 Torr oxygen was added to the IR cell and spectra were taken after 8, 24, 40, and 60 min. After *in situ* measurements the partial reduction of the Sn–Pt/SiO_2 (B) catalyst with hydrogen was also investigated. In this experiment the cell was evacuated at 10^{-3} mbar and the background spectrum was taken. Afterward the sample was kept in pure hydrogen for 1 h and evacuated and a new spectrum was measured.

The density functional approximation level with the local VWN functional and the minimal basis set was used to model the interaction of adsorbed CO molecule with a hypothetical Pt–Sn cluster. The core electrons of the metal atoms were represented by relativistic effective core potentials (ECPs). These metal atoms were positioned in order to form a small cluster on the (110) surface of the PtSn crystal according to Ref. (16). The locations of the metal atoms were fixed during the calculations, while the geometry of the CO molecule and its position relative to the metal cluster were fully optimized.

RESULTS AND DISCUSSION

In Situ Mössbauer Measurements

In studying the low temperature oxidation of carbon monoxide, both 300 and 77 K *in situ* spectra were recorded on Sn–Pt/SiO_2 (B) catalysts ((O) type (sample II-3 in Ref. 8)). The 300 and 77 K spectra measured are presented in Figs. 1A and 1B, respectively, and the corresponding data are compiled in Table 1. This table displays f_A values as well.

The 300 K spectra are the "genuine" *in situ* spectra since they were obtained under the actual reaction conditions. Consequently, the 300 K spectra reflect species formed under dynamic reaction conditions, while the 77 K spectra can be attributed to stabilized surface species. We believe that the data extracted from 77 K spectra are probably more reliable, since the probability of Mössbauer effect for different species strongly depends on the temperature.

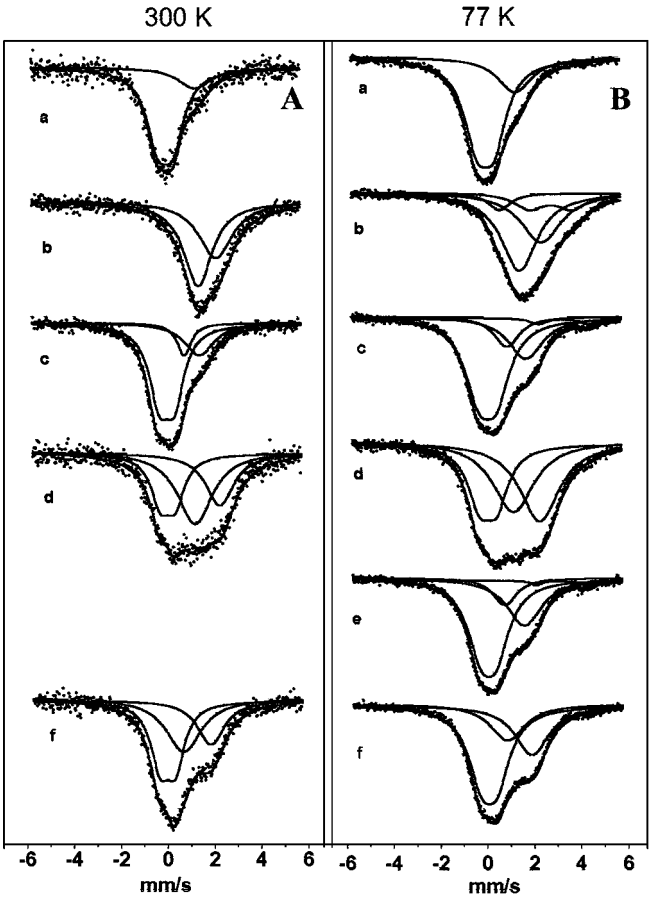

FIG. 1. Mössbauer spectra of Sn–Pt/SiO_2 (B) catalysts under different experimental conditions. (A) spectra obtained at 300 K, (B) spectra obtained at 77 K. Catalyst samples: (a) as received, (b) after reduction at 573 K in hydrogen, (c) *in situ* measurement in CO oxidation at 300 K, (d) *in situ* reduction in hydrogen at 300 K, (e) *in situ* measurement in CO oxidation at 300 K, and (f) *in situ* treatment in CO.

In our recent studies (8, 13) when fitting the Mössbauer spectra, the alloy fraction was divided into two alloy-type species with isomer shifts between 1.20–1.56 and 2.23–2.35 mm s^{-1}, respectively. Based on literature data (16–19) the former alloy species can be assigned to tin dissolved in Pt (Sn < 6 at.%) and/or to Pt_3Sn, while the latter one can be related to the tin-rich Pt_2Sn_3 and $PtSn_4$ phases (Pt–Sn(b) phase). In a recent Mössbauer spectroscopic study at 7 K in PtSn/MgO catalysts prepared using similar surface chemistry more composition ranges were distinguished (18). We admit that alloy phases with intermediate compositions can also be present in our Sn–Pt/SiO_2 catalysts. However, because of the substantial overlap of the spectral lines, we have used the parameters belonging to these two extreme compositions for the fitting procedures. Using this approach the variations in the amount of the Pt-rich and Sn-rich species can easily be followed. Therefore, in this work we also differentiate the Pt–Sn(a) and Pt–Sn(b) alloy-type species.

In the *in situ* oxidation of CO a new species with isomer shifts around 1.58–1.93 mm s^{-1} became dominant. This isomer shift is close to that of the PtSn (1 : 1) alloy species (17–19); thus this third component can be denoted as PtSn (1 : 1) alloy species thereafter. Furthermore, an additional new component arises with IS between 0.80 and 0.94 mm s^{-1} (and after a repeated CO + O_2 treatment at 0.79 mm s^{-1}, as well (see spectra e)). This value is beyond the lowest IS assigned for bimetallic tin alloys. Based on literature analogies this component can probably be assigned to Sn^{4+} (21) and can be attributed to a well-dispersed surface species, Sn^{4+}(sf), since its IS value is significantly different from that of oxidic Sn^{4+}. This type of species was also evident in our earlier studies (8, 13).

In as received Sn–Pt/SiO_2 catalysts the dominating portion of the starting sample is Sn^{4+} oxide (see spectra a in Figs. 1A and 1B). This was expected as after the preparation the sample was kept in air. The high temperature (573 K) activation in hydrogen results in the formation of bimetallic phases in overwhelming dominance (see spectra b in Figs. 1A and 1B). Similar to our recent studies (8, 13) two Pt–Sn alloy species were distinguished, PtSn(a) with IS between 1.34 and 1.37 mm s^{-1} and PtSn(b) with IS between of 2.24 and 2.41 mm s^{-1}. The Sn^{2+} and Sn^{4+} components together amount to 16% spectral area. It is worth noting that upon reduction at 573 K the Sn^{4+}(ox) species are completely absent in the spectrum recorded at 300 K. The Sn^{2+} and Sn^{4+} species may have originated from organometallic species formed at the particle peripheries and subsequently become incorporated into the support (19, 20). Another possible explanation for the presence of ionic tin compounds is that their full reduction requires a slightly higher temperature and prolonged reduction time.

From Figs. 1A and 1B it can be seen that the character of *in situ* Mössbauer spectra taken in the presence of CO + O_2 at room temperature has been completely changed compared to the reduced form of the catalyst (compare spectra b and c). The oxidative atmosphere in the presence of CO resulted in (i) oxidation of both PtSn(a) and PtSn(b) alloy species to Sn^{4+} in a high proportion and (ii) the dominance of the PtSn (1 : 1) alloy species with IS values around 1.58–1.81 mm s^{-1} (see Figs. 1A and 1B and calculated spectra c in Table 1).

The room temperature treatment in hydrogen also resulted in very pronounced changes in the composition of the catalyst. Interestingly, not only the mobile and highly reactive surface species, Sn^{4+}(sf) but also part of Sn^{4+}(ox) is reversibly transformed to the original alloy phases. The reduction of the Sn^{4+}(sf) phase is complete and the proportion of Sn^{4+}(ox) drops from 62 to 31% area in the spectrum and simultaneously the platinum-rich PtSn(a) and the tin-rich PtSn(b) components reappear in 34 and 35% relative intensity, respectively. This result indicates that 82% of the original alloy content has been restored by room

TABLE 1

Mössbauer Parameters Obtained from 77 and 300 K Spectra of (O)-Type PtSn/SiO_2 (B) Used for 300 K Oxidation of CO

Temperature of measurement:			300 K				77 K				
	Treatment	Comp:	IS	QS	FWHM	RI[a]	IS	QS	FWHM	RI[a]	$\propto f_A$
a	As received	Sn^{4+}(ox)	0.00(1)	0.65(2)	1.07(4)	82	0.00(1)	0.72(1)	1.29(1)	77	3.5
		PtSn(a)	1.37(7)	—	1.53(17)	18	1.38(2)	—	1.66(4)	23	4.7
b	570 K in H_2	Sn^{4+}(sf)					0.55(3)		0.79(14)	4	
		Sn^{2+}					2.76[b]	2.32[b]	1.38(15)	12	
		PtSn(a)	1.34(2)	—	1.44(5)	54	1.37(3)	—	1.66(16)	41	4.1
		PtSn(b)	2.24(5)	—	1.87(7)	46	2.41(6)	—	1.96(14)	42	4.8
c	300 K in $CO + O_2$	Sn^{4+}(ox)	0.00(1)	0.70(1)	1.07(2)	75	0.01(1)	0.74(1)	1.22(1)	62	3.1
		Sn^{4+}(sf)	0.80[b]	—	0.90(14)	7	0.94(2)	—	1.07(8)	11	6.1
		Sn^{2+}					3.41(2)	2.03(5)	0.81(6)	4	
		PtSn (1 : 1)	1.58(3)	—	1.45(7)	18	1.81(2)	—	1.44(6)	23	4.9
d	300 K in H_2	Sn^{4+}(ox)	−0.01(2)	0.65(2)	0.96(7)	30	0.01(1)	0.71(1)	1.03(3)	31	5.9
		PtSn(a)	1.23(4)	—	1.79(23)	43	1.24(2)	—	1.74(10)	34	4.6
		PtSn(b)	2.34(4)	—	1.53(12)	27	2.44(2)	—	1.74(5)	33	6.6
e	300 K in $CO + O_2$	Sn^{4+}(ox)					−0.04(2)	0.66(1)	1.16(2)	58	
		Sn^{4+}(sf)					0.79(3)		1.03(8)	10	
		Sn^{2+}					3.31(2)	2.11(4)	0.51(6)	2	
		PtSn (1 : 1)					1.68(2)	—	1.57(4)	29	
f	300 K in CO	Sn^{4+}(ox)	−0.06(1)	0.65(1)	0.97(3)	47	−0.05(1)	0.65(1)	1.10(2)	50	4.7
		Sn^{4+}(sf)	0.80[b]	—	1.60(19)	28	0.88[b]	—	1.46(10)	21	(3.0)
		PtSn (1 : 1)	1.91(2)	—	1.40(8)	25	1.93(1)	—	1.52(3)	30	5.1

Note. IS, isomer shift, relative to SnO_2, mm/s; QS, quadrupole splitting, mm/s; FWHM, linewidth, mm/s; RI, relative intensity %, $\propto f_A$, $= -d \ln(A_{300}/A_{77})/dT \times 10^{-3}$, where A_{300} and A_{77} are the actual absorption areas of components in the spectra recorded at 300 and 77 K, respectively.

[a] RI is a derived parameter with an error summarized from those of the components (base line, intensity, FWHM—it is estimated at ca. 10 relative %).

[b] Constrained parameters.

temperature hydrogen treatment (compare samples b and d). After rereduction the Pt–Sn (1 : 1) alloy phase was completely converted back to the original alloy phases.

Consequently, the intimate contact between Sn and Pt, in both the reduced and the working catalyst containing supported alloy-type nanoclusters, is convincingly demonstrated by the *room temperature* regeneration in hydrogen. This regeneration clearly proves the $Sn^{4+} \leftrightarrow Sn^0$ transformation at room temperature in both PtSn(a) and PtSn(b) bimetallic species. In addition, it is worth comparing the effects of 573 K and room temperature reactivation in hydrogen: the corresponding IS values (i.e., their compositions) of PtSn(a) and PtSn(b) are very close and even their proportion is the same.

In a subsequent room temperature $CO + O_2$ treatment partial reoxidation of Sn to Sn^{4+}(ox) and Sn^{4+}(sf) was evidenced again with simultaneous disappearance of both PtSn(a) and PtSn(b) components in the catalyst (see spectrum e in Fig. 1B). This experiment provided additional proof for the reversibility of nanocluster reconstruction.

However, the treatment in pure CO (see spectrum f) cannot reduce the oxide phases into the alloy components. This treatment resulted in only slight alteration in the ratio of the Sn^{4+}(ox) and Sn^{4+}(sf) phases.

The calculated f_A values are in correspondence with the considerations given under Experimental. Please note that cases with RI < 10% possessed relatively large fit uncertainty and were not considered. For interpretation, low values are characteristic of strong ionic bonds (e.g., for a separate SnO_2 phase a value of 1.0×10^{-3} is obtained (19)). However, in large organic complex molecules with looser bonds f_A values close to 10^{-2} can be obtained (22). Strong interaction of tin with oxygen is reflected in the $f_A \approx 3 \times 10^{-3}$ value estimated for Sn^{4+}(ox) after $CO + O_2$ treatments. In contrast, after room temperature reactivation in hydrogen (see sample d), Sn^{4+}(ox) exhibits a significantly larger f_A value (5.87×10^{-3}) than in samples c or a. Further, the surface character of Sn^{4+}(sf) is reflected in large f_A values (6.08×10^{-3}) after $CO + O_2$ treatments. In a comparison of PtSn(a) and PtSn(b) components the f_A values provide further insight; i.e., for the tin-depleted PtSn(a) component, a relatively low f_A value ($\propto f_A = 4.1$–4.6×10^{-3}) is obtained, indicating the incorporation of tin into the core of bimetallic particles. Whereas, tin in PtSn(b) is more loosely bound as $f_A \approx 4.8$–6.5×10^{-3} indicates. It is worth noting that when the IS values were constrained the accuracy of these calculations strongly decreases. This is probably, the case for Sn^{4+}(sf) in sample f.

Based on the assignment discussed above it is suggested that the primary interaction with the CO–oxygen mixture leads to a strong reconstruction of supported Sn–Pt nano-clusters. The reconstruction is mainly related to the

oxidation of metallic tin to Sn^{4+} in both the surface layer and the bulk of the nanoparticles. The net result of this reconstruction is the enrichment of tin in the surface layer of the bimetallic particles in the form of Sn^{4+}. In the working catalyst at least two forms of Sn^{4+} can be differentiated, i.e., (i) a more stable one, Sn^{4+}(ox) with isomer shift around zero, and a mobile one, Sn^{4+}(sf) with IS = 0.79–0.94 mm s^{-1}. The results indicate also that during *in situ* CO oxidation a third new species, i.e., the Pt–Sn (1 : 1) alloy with IS = 1.4–1.7 mm s^{-1}, has been formed.

The oxidation during the CO + O_2 reaction does not result in extended separation of the oxidized Sn^{4+} forms, since both the Sn^{4+}(ox) and the Sn^{4+}(sf) components are readily reconverted in hydrogen at room temperature to PtSn(a) and PtSn(b) phases. During the CO + O_2 reaction, the surface of the nanoparticles containing both mono- and bimetallic metallic sites are probably covered mostly by Sn^{4+} species, while providing simultaneous access to CO both on free platinum sites and on the Pt–Sn (1 : 1) alloy.

In Situ FTIR Measurements

Three different catalysts were investigated by *in situ* FTIR measurements: Pt/SiO_2, Sn–Pt/SiO_2 (A), and Sn–Pt/SiO_2 (B). FTIR spectra of chemisorbed CO on different catalysts are shown in Fig. 2-I. The characteristic frequencies of the linear and bridged CO bands are summarized in Table 2. As emerges from these data the addition of tin into the Pt/SiO_2 catalyst decreases slightly both the frequency and the intensity of the linear CO bands. On the parent Pt/SiO_2 and the Sn–Pt/SiO_2 (A) catalyst the bridged CO band appeared around 1865 cm^{-1}. Due to the relatively high tin loading no bridged CO band was observed on Sn–Pt/SiO_2 (B) catalyst.

Data obtained on the parent Pt/SiO_2 catalyst are in a good agreement with literature data (23–25). The observed behavior of our Sn–Pt/SiO_2 catalyst is characteristic for tin-modified supported platinum catalysts (25–27) and has been attributed to the dilution of the platinum surface with tin.

FTIR spectra of adsorbed CO in the presence of oxygen are presented in Fig. 2-II. As emerges from these results in the parent platinum catalyst the addition of oxygen to CO had no detectable changes in the spectrum. However, significant alteration can be seen in the spectra of both Sn–Pt/SiO_2 catalysts. The shift in the CO band frequencies indicates that in the presence of oxygen the surface composition of the supported tin–platinum nanocluster has been altered and the extent of these changes depends on the Sn/Pt ratio (compare A and B samples).

After addition of oxygen catalyst sample A strongly resembles the parent platinum catalyst. On this sample the CO frequency of linear CO band was shifted toward the high frequency region (Δ_{CO} = 4 cm^{-1}) and the intensity of the bridged CO band increased significantly. In B the band position of linear CO is also shifted (Δ_{CO} = 6 cm^{-1}) and there is a noticeable half-width broadening after exposure to oxygen (see Fig. 2). The analysis of band intensities indicates also that substantial intensity changes (around 25%) can only be seen in B (see Table 2 and compare band intensities of samples B, A, and parent Pt/SiO_2 catalyst in both the absence and presence of oxygen). Consequently, pronounced replacement of chemisorbed CO by oxygen can only be expected in sample B.

The 1 h room temperature hydrogen treatment of sample B used in CO oxidation (Table 2, Experiment 3) resulted in a decrease in the CO band frequency from 2076 to 2071 cm^{-1}; however, the original band intensity was not restored. This new frequency value is very close to that measured on the fully reduced sample (B) (see Table 2, Experiment 1). Hence, the room temperature reduction of the *in situ* formed tin–oxide phase has been proven by

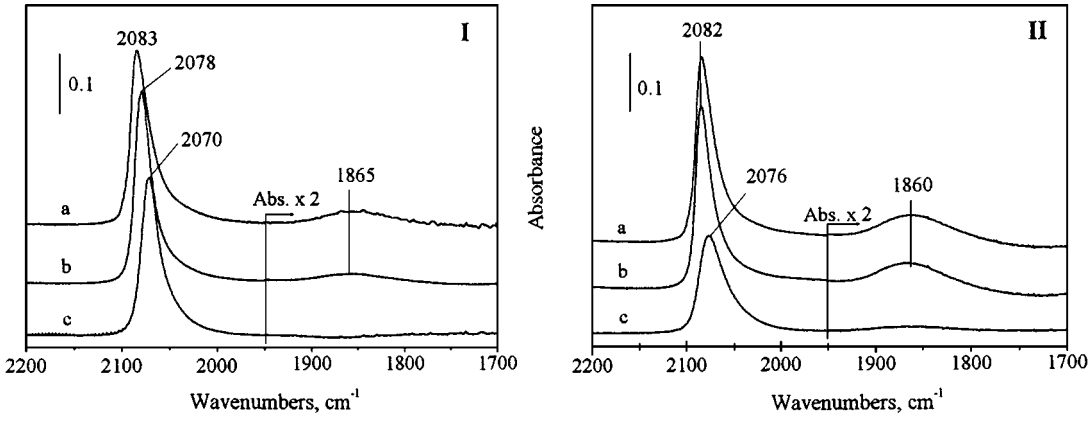

FIG. 2. FTIR spectra of chemisorbed CO on different catalysts. (I) Spectra measured in the presence of pure CO (P_{CO} = 10 Torr) (spectra were taken after equilibration for 40 min). (II) spectra measured in the presence of CO + O_2 mixture (P_{CO} = 10 Torr, P_{O_2} = 5 Torr) (spectra were taken after equilibration for 60 min). Catalysts samples: (a) Pt/SiO_2, (b) Sn–Pt/SiO_2 (A), (c) Sn–Pt/SiO_2 (B).

TABLE 2

Summary of *in Situ* FTIR Experiments: Frequency and Intensity Changes of the Linear CO Adsorption Band under Conditions of CO Oxidation at Room Temperature

		Catalysts					
		Pt/SiO_2		Sn–Pt/SiO_2(A)		Sn–Pt/SiO_2 (B)	
No.	Experimental condition	CO^a_{lin} cm^{-1}	CO^a_{br} cm^{-1}	CO^a_{lin} cm^{-1}	CO^a_{br} cm^{-1}	CO^a_{lin} cm^{-1}	CO^a_{br} cm^{-1}
1	Adsorption of CO	2083 (9.12)	1865 (0.88)	2078 (8.99)	1865 (0.58)	2070 (8.18)	n.m. (n.m.)
2	In the presence of $CO + O_2$ mixture[b]	2082 (9.30)	1865 (1.78)	2082 (8.46)	1860 (1.58)	2076 (6.66)	1860 (.57)
+3	After room temperature reduction of sample No. 2 in H_2	—	—	—	—	2071 (6.15)	1860 (n.m.)
4	In the presence of $CO + O_2$ mixture[c]	—	—	—	—	2083 (n.d.)	1860 (n.m.)

[a] Frequency and normalized intensity data (the latter are given in parentheses).
[b] Addition of CO first;
[c] introduction of oxygen first. Spectra measured after 40 min of equilibration; n.d., not determined; n.m., not measurable.

in situ FTIR measurements, however, as emerges from corresponding band intensities (see Table 2) the reduction is only partial. Full reduction would require higher reduction temperature.

Results presented in Table 2 indicate also that the reversal of the addition of reactant, i.e., the addition of oxygen, first has resulted in substantial differences in the FTIR spectra of chemisorbed CO. These experiments were performed on Pt–Sn/SiO_2 (B) catalysts by addition of oxygen first and subsequent introduction of CO after 5 minutes (see Experiment No. 4 in Table 2). In this sample the low frequency CO band at 2070 cm^{-1} disappeared and the spectrum strongly resembled that of the parent platinum ($(CO)_{lin}$ = 2083 cm^{-1}, $(CO)_{br}$ = 1855 cm^{-1}). This result indicates that upon contact with pure oxygen, fast oxidation of supported bimetallic nanoclusters takes place. The oxidation leads to rapid segregation of phases and the subsequent addition of CO cannot restore the surface composition formed in the presence of $CO + O_2$ mixture (compare Experiments 2 and 4). However, it must be emphasized that the above segregation leads to the reappearance of pure Pt sites ($(CO)_{lin}$ = 2083 cm^{-1}, $(CO)_{br}$ = 1865 cm^{-1}). Preliminary catalytic experiments showed also that the activity of the Sn–Pt/SiO_2 catalyst was extremely low when the catalyst was preoxidized, i.e., when oxygen was introduced first.

Difference spectra obtained on Sn–Pt/SiO_2 (B) catalysts in the presence of $CO + O_2$ mixture and in pure CO are shown in Fig. 3. The analysis of difference spectra provided further insight into the changes induced by addition of oxygen. As emerges from Fig. 3 the intensity of the band at 2068–2069 cm^{-1} diminishes, while that of the band at 2082–2085 cm^{-1} increases. A similar trend was also evidenced in catalyst sample A, where diminishing and increasing the band intensities at 2074 and at 2085 cm^{-1}, respectively, has been also evidenced.

Figure 3 reveals also the time dependence of changes induced by the addition of oxygen. After 8 min only a minor alteration can be seen; however, after 25 min there are no further measurable changes in the band intensities at both 2069 and 2085 cm^{-1}. Parallel to the above changes a very pronounced increase was also observed in the intensities of the $(CO)_{br}$ band at 1860 cm^{-1}. This change appeared to be continuous in the whole time interval. These results might indicate that the bridged CO band is more sensitive in reflecting minor surface reconstruction than the linear one.

The above changes in the difference spectra indicate that upon introduction of the CO + oxygen mixture the

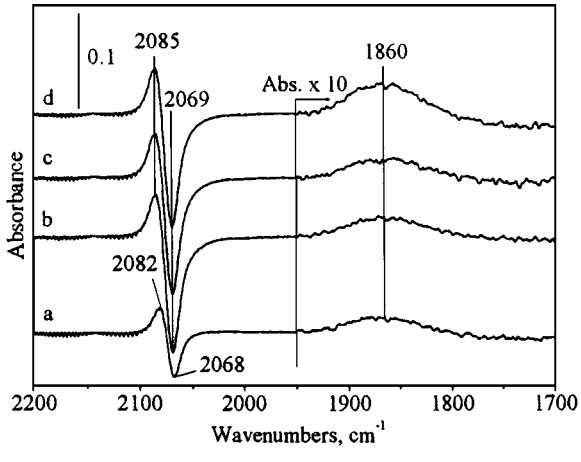

FIG. 3. Time-dependent difference FTIR spectra of chemisorbed CO on Sn–Pt/SiO_2 (B) catalysts. Difference spectra induced by addition of oxygen after (a) 8 min, (b) 25 min, (c) 40 min, and (d) 60 min.

supported Pt–Sn alloy phases are transformed and segregated and this is a time-dependent process; however, the rate of these surface transformations is relatively fast. The net results of changes induced by oxygen are as follows: (i) the number of bimetallic tin-rich alloy sites at 2069 cm^{-1} diminishes, and (ii) and number of pure Pt sites that adsorb CO around 2085 cm^{-1} increases. In sample B the extent of the formation of segregated Pt sites is so pronounced that the CO band of the bridged CO appears at 1860 cm^{-1}.

Based on the analysis of the intensity ratios (see Fig. 3) the loss of the bimetallic sites is more pronounced than the gain in the monometallic one. It should be emphasized that the formation of pure Pt sites has been evidenced on both Pt–Sn catalysts; i.e., the site separation is characteristic for both platinum-rich and tin-rich alloy phases. These results are in good accordance with the results of Mössbauer spectroscopy, where in the presence of oxygen the transformation of both PtSn(a) and PtSn(b) alloy species has been shown and the formation of tin oxide-like phases has been demonstrated (see Table 1). Consequently, based on results of *in situ* FTIR we can further substantiate the PtSn $\rightarrow$ Sn^{4+} + Pt conversion taking place in the low temperature CO oxidation. However, at this moment it is difficult to differentiate between pure Pt sites and accessible Pt sites in the PtSn (1 : 1) species formed.

Both Mössbauer and FTIR spectroscopy provided further evidences with respect to the low temperature partial rereduction of tin-oxide like species formed during CO oxidation (see results given in Tables 1 and 2). These results indicate that the surface reaction, Sn^{4+} + Pt $\rightarrow$ PtSn, takes also place at room temperature; i.e., the changes in the surface composition are reversible. This reversibility can only be achieved if the segregation described above is within the supported nanoparticle, i.e., when surface reactions involved in CO oxidation do not result in formation of separate Pt and tin-oxide phases on the silica support.

Time-on-Stream Experiments

The results of Mössbauer spectroscopy indicated that the formed Sn^{4+}(ox) and Sn^{4+}(sf) components can be readily reconverted in hydrogen at room temperature to the parent PtSn(a) and PtSn(b) alloy species. For this reason it was interesting to check the possibility of regenerating the Sn–Pt/SiO_2 catalyst at room temperature with hydrogen. These results are shown in Fig. 4.

Prior to the first experiment the Sn–Pt/SiO_2 catalyst was treated at 613 K in a hydrogen flow (60 ml/min). Omitting this preactivation the catalyst showed no activity at room temperature. In the first oxidation experiment after 2 h of TOS the activity of the catalyst dropped from 86 to 24% conversion. After the first experiment the reactor was flushed with helium for 30 min and hydrogen flow (60 ml/min) was introduced for 10 min. Afterward

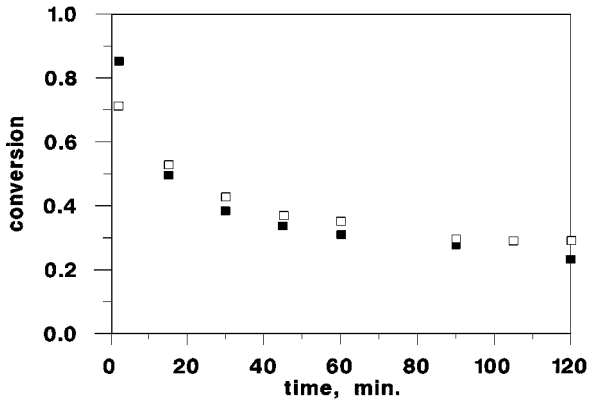

FIG. 4. Regeneration of Sn–Pt/SiO_2 (B) catalyst with hydrogen at room temperature. Time-on-stream experiments: (■) first run, (□) second run after treatment with hydrogen for 10 min.

the reactor was purged again with helium for 30 min and the CO oxidation restarted again. This result show that due to the above treatment with hydrogen, the activity of the catalyst increased up to 71% conversion and after 90 min TOS the activity stabilized at the 30% conversion level. In these two experiments there was no substantial difference in the rate of deactivation of the Sn–Pt/SiO_2 catalyst. Using Vorhies equation (28), within the experimental error, there were no significant differences in the calculated deactivation parameters n (n = 0.31 and 0.35 for the first and second experiment, respectively). Similar results, i.e., deactivation and reactivation patterns, were also obtained when the O_2/CO volume ratio was increased from 0.5 to 1.

The most important messages from these TOS experiments are as follows: (i) room temperature treatment in hydrogen almost fully restores the activity of Sn–Pt/SiO_2 catalysts, and (ii) there is no measurable differences in the aging properties of fresh and regenerated catalysts.

The above TOS results are in good accordance with our earlier finding (8). In a recent report it has been demonstrated that although the Sn–Pt/SiO_2 catalysts are highly active in low temperature oxidation of CO, the catalysts are not stable; they deactivate (8). The extent of deactivation depended on both the Sn/Pt ratio and the type of Sn–Pt/SiO_2 catalysts used (8).

Summing up the results of TOS experiments the reducibility of the Sn^{4+}(ox) and Sn^{4+}(sf) components of the working Sn–Pt/SiO_2 catalyst with hydrogen at room temperature have been unambiguously demonstrated. However, further experiments will be needed to elucidate the character and the origin of the deactivation of Sn–Pt/SiO_2 catalysts in low temperature CO oxidation.

Computer Modeling

According to the results of *in situ* Mössbauer spectroscopy the formation and stabilization of the PtSn (1 : 1) alloy phase cannot be ruled out under conditions of room

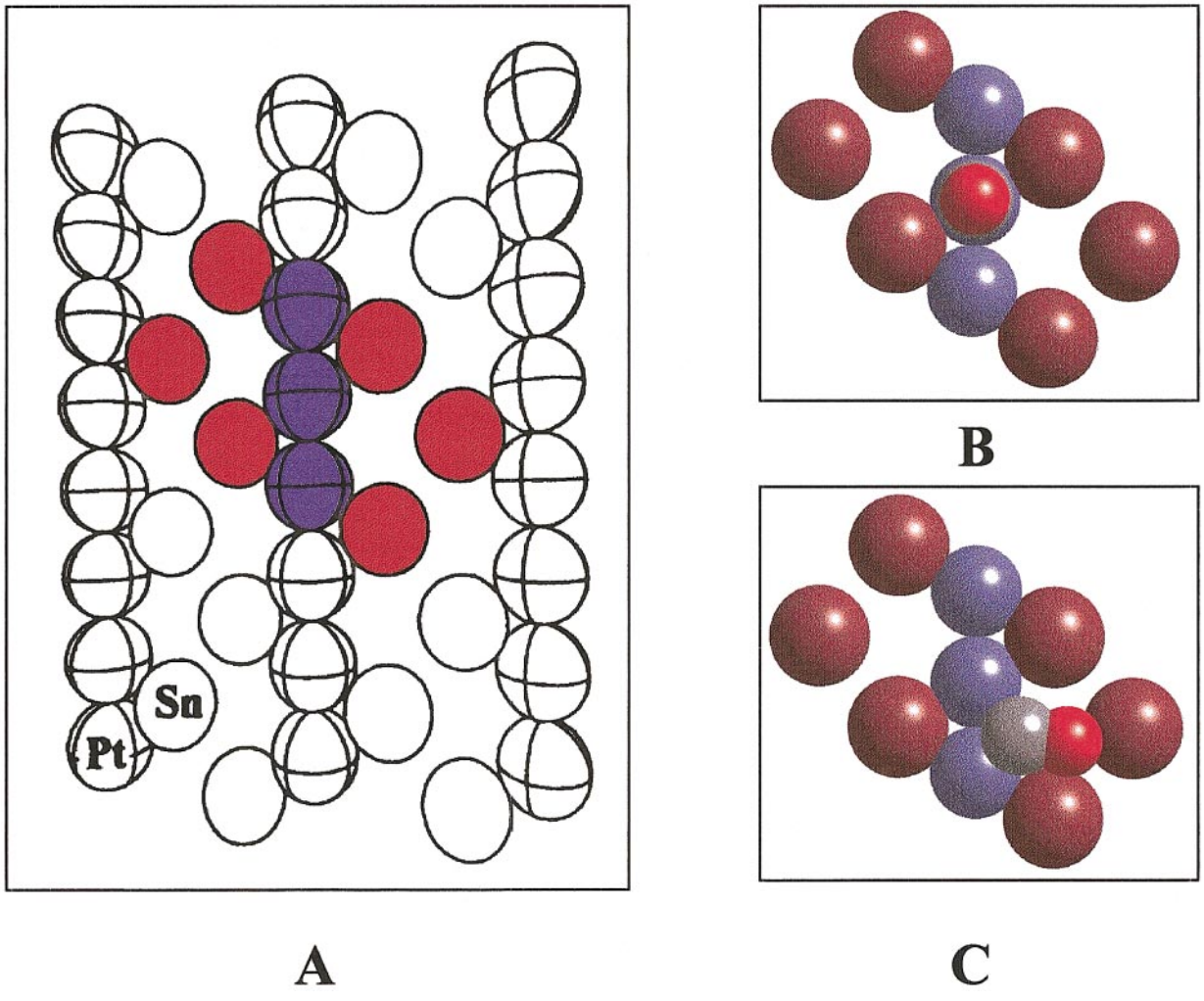

FIG. 5. Alignment of the CO molecule chemisorbed at the cluster of the (110) surface of the PtSn (1 : 1) alloy phase, (A) the (110) surface of PtSn (1 : 1) alloy phase (Pt, blue; tin, red); (B) linear coordination of CO on the cluster of metal atoms; (C) bent coordination of CO on the cluster of metal atoms (carbon, red; oxygen, gray). The bent structure is required for the activation of the CO molecule.

temperature CO oxidation. Based on these results one of the most active surfaces of the PtSn (1 : 1) alloy phase, the (110) surface, was chosen to model the interaction of the CO molecule with the metal surface (16). The computer modeling and the related calculations were made on density functional level. In this model a small cluster of the (110) surface of the PtSn phase (16) as shown in Fig. 5A was selected in order to calculate and investigate the interaction of the CO molecule with the metal surface.

Two alignments of the CO molecule relative to the metal cluster were examined, for total charges $N = 0, +4$. For the linear alignments, the CO molecule is perpendicular with the surface and no O $\cdots$ Sn interaction is possible. In contrast, for the bent structures, the oxygen atom of the CO molecule chemisorbed on the Pt is near to a tin atom, allowing interaction between them. The structures of the above alignments are shown in Figs. 5B and 5C, for neutral surface.

The results of the above calculations for the CO molecule and for its interaction with N-fold charged metal clusters are presented in Table 3, for $N = 0$ and $+4$. These results show that for these interactions the charge of the system has less effect on the C≡O bond than the alignment of the CO molecule relative to the metal cluster. However, it is clearly shown that the alignment strongly affects the C≡O bond, as the bent structures have more significant effect on the bond lengths and bond orders than the linear structures. On the other hand, it is also demonstrated that for the neutral system the linear structure is energetically more stable than the bent alignment, while the opposite relationship holds for the charged one. These

TABLE 3

Bond Lengths and Mayer Bond Orders of the C≡O Bond in the Carbon-Monoxide Molecule and in CO + (Cluster)^N Complexes and the Energy Differences between Bent and Linear Structures ($\Delta E = E_{bent} - E_{linear}$)

	Bond length (Å)		Mayer bond order		ΔE
	Linear	Bent	Linear	Bent	(kcal/mol)
CO	1.317		2.46		
CO + (cluster)^0	1.338	1.415	2.02	1.42	205.41
CO + (cluster)$^{4+}$	1.324	1.406	2.18	1.42	−34.89

results support the assumption that on the uncharged cluster the chemisorbed CO molecule is perpendicular with the metal surface with no O···Sn interaction. If the surface is charged, the alignment of the molecule is bent and the C≡O bond is weakened because of the involvement of Sn^{4+}–Pt ensemble site in this interaction. Consequently, these calculations strongly support the relevance of our hypothesis with respect to the involvement of Sn^{4+}–Pt ensemble sites and the C≡O–Sn^{4+} interaction in the increased activity of our alloy-type Sn–Pt/SiO_2 catalysts in low temperature CO oxidation (8).

Finally, we would like here to refer to our working hypothesis with respect to the possibility of using our Sn–Pt/SiO_2 catalysts in CO oxidation (8). The working hypothesis was based on the involvement of the Sn^{4+}–Pt ensemble sites in the activation of both the carbonyl group in unsaturated aldehydes and the CO molecule (8). All of the results presented here and earlier (8) are in agreement with our hypothesis. However, there is one significant difference between these two processes.Using Sn–Pt/SiO_2 catalysts high selectivity for the formation of unsaturated alcohol was obtained at Sn/Pt (at./at.) > 1.0. Contrary to that in CO oxidation the best results were attained at Sn/Pt (at./at.) = 0.4–0.7. The above difference can be explained by a specific need for surface sites to suppress the readsorption of formed unsaturated alcohol. The suppression of the readsorption of unsaturated alcohol can only be achieved if platinum is strongly diluted by metallic tin; i.e., the surface concentration of the tin-rich alloy phase is relatively high. Therefore this reaction requires Sn–Pt/SiO_2 catalysts with a high Sn/Pt (at./at.) ratio.

In CO oxidation we do not need tin-rich alloy sites for adsorption of CO. The chemisorption of CO takes place on Pt sites formed *in situ*. It is the reason that the segregation process described above is not harmful for the reaction. Contrary to that, it is very beneficial for the formation of Sn^{4+}–Pt ensemble sites. However, at high Sn/Pt (at./at.) ratio (Sn/Pt > 0.9) the formed Pt sites might be covered by the inactive Sn^{4+}(ox) phase formed *in situ*. In this way the number of sites required for CO chemisorption decreases and the rate of CO oxidation diminishes on Sn–Pt/SiO_2 catalysts with Sn/Pt > 0.9.

SUMMARY

Upon using Mössbauer spectroscopy the active participation of tin in our Sn–Pt/SiO_2 catalysts was demonstrated in the low temperature CO oxidation. The *in situ* measurements revealed that the enrichment of tin in the surface layers of the bimetallic nanoparticles plays a crucial role. The reversible interconversion of PtSn ↔ Sn^{4+} + Pt was demonstrated in the low temperature CO oxidation reaction and the surface character of the involved species is proposed. The above interconversion was also supported by *in situ* FTIR measurements. In *in situ* experiments it was demonstrated for the first time that both metallic and ionic species can coexist in the same supported particle (nanocluster) and both the parent alloy species and the newly formed ionic and metallic species are highly mobile and reactive even at room temperature. Based on these results we suggest that in the presence of room temperature CO oxidation the supported bimetallic nanocluster is oxidized and strongly reconstructed. The net result of these transformations is the formation of the following species or sites:

(i) Tin oxide phase (IS = 0.0 mm s^{-1}, QS = 0.6–0.7 mm s^{-1});

(ii) Free platinum sites (CO_{lin} = 2085 cm^{-1}, CO_{br} = 1860 cm^{-1});

(iii) Highly mobile Sn^{4+}(sf) phase (IS = 0.79–0.94 mm s^{-1}); and

(iv) New alloy phase, Pt–Sn (1 : 1) (IS = 1.6–1.9 mm s^{-1}).

The schematic view of the supported nanocluster after its reconstruction in the presence of CO and O_2 mixture is shown in Scheme 1.

It is suggested that the oxidation of CO takes place at the Sn^{4+}–Pt ensemble sites, formed *in situ*. In the formation of these ensembles the involvement of the (110)

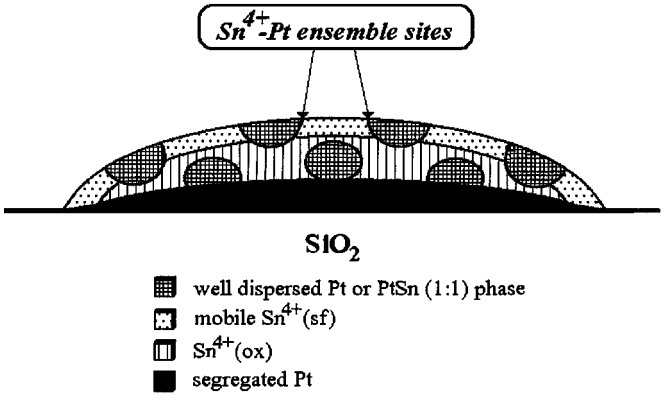

SCHEME 1

sites of the SnPt (1:1) alloy species has also been proposed. The possible mode of the activation of the CO molecule on the above sites was also modeled and calculated. The results of time-on-stream catalytic experiments are in full agreement with the results of *in situ* spectroscopic measurements.

ACKNOWLEDGMENTS

Partial financial help from OTKA (OTKA Grants 25732 and 32065) is greatly acknowledged. Thanks also for the pertinent remarks of the referees.

REFERENCES

1. Sárkány, J., Bartók, M., and Gonzales, R., *J. Catal.* **81**, 347 (1983).
2. Yu Yao, Y. F., *J. Catal.* **87**, 152 (1984).
3. Gardner, S., Hoflund, G. B., Davidson, M. R., and Schryer, D. R., *J. Catal.* **115**, 132 (1989).
4. Gangel, N. D., Gupta, M., and Iyer, R. M., *J. Catal.* **126**, 13 (1990).
5. Grass, K., and Linz, H.-G., *J. Catal.* **172**, 446 (1997).
6. Bond, G. C., Molloy, L. R., and Fuller, M. J., *J.C.S. Chem. Comm.* 796 (1975).
7. Sheintuch, M., Schmidt, J., Lechtman, Y., and Yahav, G., *Appl. Catal.* **49**, 55 (1989).
8. Margitfalvi, J. L., Borbáth, I., Hegedűs, M., Tfirst, E., Gőbölös, S., and Lázár, K., *J. Catal.* **196**, 200 (2000).
9. Margitfalvi, J. L., Tompos, A., Kolosova, I., and Valyon, J., *J. Catal.* **174**, 246 (1998).
10. Margitfalvi, J. L., Borbáth, I., Tfirst, E., and Tompos, A., *Catal. Today* **43**, 29 (1998)
11. Margitfalvi, J. L., Borbáth, I., Hegedűs, M., Gőbölös, S., and Lónyi, F., *React. Kinet. Catal. Lett.* **68**, 133 (1999).
12. Vértes, Cs., Tálas, E., Czakó-Nagy, I., Ryczkovski, J., Gőbölös, S., Vértes, A., Margitfalvi, J., *Appl. Catal.* **68**, 149 (1991).
13. Margitfalvi, J. L., Vankó, Gy., Borbáth, I., Tompos, A., and Vértes, A., *J. Catal.* **190**, 474 (2000).
14. Lázár, K., Matusek, K., Mink, J., Dobos, S., Guczi, L., Vizi-Orosz, A., Markó, L., and Reiff, W. M., *J. Catal.* **87**, 163 (1984).
15. Karge, H. G., Hunger, M., Beyer, H. K., *in* "Catalysis and Zeolites" (J. Weitkamp and L. Puppe, Eds.), p. 198. Springer-Verlag, Berlin, 1999.
16. Kappenstein, Ch., Guérin, M., Lázár, K., Matusek, K., and Paál, Z., *J. Chem. Soc., Faraday Trans.* **94**, 2463 (1998).
17. Charlton, J. S., Cordey-Hayes, M., and Harris, I. R., *J. Less-Common Metals* **20**, 105 (1970).
18. Stievano, L., Wagner, F. E., Calogero, S., Recchia, S., Dossi, D., and Psaro, R., *Stud. Surf. Sci. Catal.* **130**, 3903 (2000).
19. Hobson, M. C., Goresh, S. L., and Khare, G. P., *J. Catal.* **142**, 641 (1993).
20. Cortright, R. D., and Dumesic, D. A., *J. Catal.* **148**, 771 (1994).
21. Kuznetsov, V. I., Belyi, A. S., Yurchenko, E. N., Smolikov, D. M., Protasova, M. T., Zatolokina, E. V., and Duplyakin, V. K., *J. Catal.* **99**, 159 (1986).
22. Lázár, K., Szeleczky, A. M., Mal, N. K., Ramaswamy, A. V., *Zeolites* **19**, 123 (1997).
23. Sheppard, N., and Nguyen, T. T., *in* "Advances in Infrared and Roman Spectroscopy" (R. G. H. Clark and R. E. Hester, Eds.), Vol. 5, p. 67. Heyden, London, 1978.
24. Kappers, M. J., and van der Mass, J. H., *Catal. Lett.* **10**, 365 (1991).
25. Menorval, L.-C., Chaqroune, A., Coq, B., and Figueras, F., *J. Chem. Soc., Faraday Trans.* **93**, 3715 (1997).
26. Bateein, A. G. T. M., Toolenaar, F. J. C. M., and Ponec, V., *J. Catal.* **90**, 88 (1984).
27. Artega, G. J., Anderson, J. A., and Rochester, C. H., *J. Catal.* **184**, 268 (1999).
28. Voorhies, A., *Ind. Eng. Chem.* **37**, 318 (1945).